Atmos. Chem. Phys., 11, 1295–1311, 2011
www.atmos-chem-phys.net/11/1295/2011/
doi:10.5194/acp-11-1295-2011

Atmospheric Chemistry and Physics

Assessment of the CALIPSO Lidar 532 nm attenuated backscatter calibration using the NASA LaRC airborne High Spectral Resolution Lidar

R. R. Rogers, C. A. Hostetler, J. W. Hair, R. A. Ferrare, Z. Liu, M. D. Obland, D. B. Harper, A. L. Cook, K. A. Powell, M. A. Vaughan, and D. M. Winker

NASA Langley Research Center, Hampton, VA 23681, USA

Received: 3 August 2010 – Published in Atmos. Chem. Phys. Discuss.: 18 November 2010
Revised: 26 January 2011 – Accepted: 4 February 2011 – Published: 15 February 2011

Abstract. The Cloud-Aerosol Lidar with Orthogonal Polarization (CALIOP) instrument on the Cloud-Aerosol Lidar and Infrared Pathfinder Satellite Observations (CALIPSO) spacecraft has provided global, high-resolution vertical profiles of aerosols and clouds since it became operational on 13 June 2006. On 14 June 2006, the NASA Langley Research Center (LaRC) High Spectral Resolution Lidar (HSRL) was deployed aboard the NASA Langley B-200 aircraft for the first of a series of 86 underflights of the CALIPSO satellite to provide validation measurements for the CALIOP data products. To better assess the range of conditions under which CALIOP data products are produced, these validation flights were conducted under both daytime and nighttime lighting conditions, in multiple seasons, and over a large range of latitudes and aerosol and cloud conditions. This paper presents a quantitative assessment of the CALIOP 532 nm calibration (through the 532 nm total attenuated backscatter) using internally calibrated airborne HSRL underflight data and is the most extensive study of CALIOP 532 nm calibration. Results show that HSRL and CALIOP 532 nm total attenuated backscatter agree on average within $2.7\% \pm 2.1\%$ (CALIOP lower) at night and within $2.9\% \pm 3.9\%$ (CALIOP lower) during the day, demonstrating the accuracy of the CALIOP 532 nm calibration algorithms. Additionally, comparisons with HSRL show consistency of the CALIOP calibration before and after the laser switch in 2009 as well as improvements in the daytime version 3.01 calibration scheme compared with the version 2 calibration scheme. Potential biases and uncertainties in the methodology relevant to validating satellite lidar measurements with an airborne lidar system are discussed and found to be less than $4.5\% \pm 3.2\%$ for this validation effort with HSRL. Results from this study are also compared with prior assessments of the CALIOP 532 nm attenuated backscatter calibration.

Correspondence to: R. R. Rogers
(raymond.r.rogers@nasa.gov)

1 Introduction

The Cloud-Aerosol Lidar and Infrared Pathfinder Satellite Observations (CALIPSO) satellite was launched in April 2006 (Winker et al., 2010). The main objective of the CALIPSO mission is to provide a global, multi-year data set of cloud and aerosol spatial and optical properties from which to assess uncertainties of aerosol direct and indirect effects on climate forcing and cloud-climate feedback (Winker et al., 2007, 2009). To address this objective, the primary payload on the CALIPSO satellite is a two-wavelength and polarization-sensitive elastic backscatter lidar, the Cloud-Aerosol Lidar with Orthogonal Polarization (CALIOP) instrument. Since becoming operational in June 2006, CALIOP has provided unprecedented observations of aerosols and clouds in the atmosphere. This paper presents a quantitative assessment of the 532 nm calibration by comparing CALIOP total attenuated backscatter profiles with coincident measurements acquired by the NASA Langley Research Center (LaRC) airborne High Spectral Resolution Lidar (HSRL).

Since the launch of CALIPSO, several studies have been conducted validating the CALIOP data products (Mona et al., 2009; Mamouri et al., 2009; Kim et al., 2008). Some promising results were also published by McGill et al. (2007) qualitatively comparing measurements from CALIOP to the Cloud Profiling Lidar (CPL) deployed on the ER-2 aircraft.

Published by Copernicus Publications on behalf of the European Geosciences Union.

McGill et al. (2007) examined the vertical distribution of clouds measured coincidently by the two instruments and assessed the minimum detectable backscatter from CALIOP. However, it concerned only a few profile comparisons showing quantitative agreement but does not provide a comprehensive quantitative assessment of CALIOP calibration accuracy. Furthermore, the CPL attenuated backscatter must be calibrated in the same manner as CALIOP while the internal calibration of the HSRL aerosol backscatter provides a truly independent calibration assessment.

The airborne HSRL, developed by NASA LaRC (Hair et al., 2008), has been deployed on ten field experiments to-date, logging over 800 h on 240 flights of the LaRC King Air B-200 aircraft. Many of these ten field missions have included CALIOP validation flights. The HSRL technique (Shipley, 1983; Piironen and Eloranta, 1994; Hair et al., 2001) allows the airborne HSRL used in this study to independently measure the aerosol backscatter and extinction profiles at 532 nm. The airborne HSRL also measures backscatter at 1064 nm using the standard backscatter technique and is polarization sensitive at both 532 and 1064 nm. The data products from the airborne HSRL are produced at high accuracy, with no assumptions in the calibration and few assumptions in the aerosol retrieval algorithms, and thereby offer an accurate and completely independent means by which to validate CALIOP data products. Because of the importance of the 532 nm total attenuated backscatter calibration, this paper focuses solely on this fundamental product. This paper also establishes a paradigm for validation of satellite lidars and other spaceborne instruments that provide nadir-only measurements: a systematic series of aircraft flights along the satellite track employing instruments with appropriate sampling geometries and measuring techniques to get an accurate and statistically significant database to validate the satellite products. HSRL validation of the CALIOP level 1 1064 nm attenuated backscatter and level 2 products are the subjects of future publications.

The outline of this paper is as follows. An overview of the HSRL validation flights are discussed in Sect. 2. Section 3 describes the CALIOP and HSRL measurements and calibrations of 532 nm attenuated backscatter, as well as the conditioning of the HSRL attenuated backscatter to the CALIOP reference altitude. The potential biases and uncertainties in this comparison methodology are examined in Sect. 4. Section 5 presents the results of the comparison, which are discussed in the context of the CALIOP calibration in conclusion Section (Sect. 6).

2 HSRL validation flights

The HSRL has completed 86 successful validation underflights of the CALIPSO satellite through 2009, acquiring 116 flight hours of data along CALIPSO orbit tracks. The average time that HSRL spent along each CALIPSO track was 1.4 h $\pm$ 0.8 h. In this time, the HSRL covers an average of 385 km along track per flight at an average ground speed of 110 m/s. Figure 1 shows the locations of the CALIOP validation flight tracks flown by the airborne HSRL. These flights cover a wide seasonal and latitude range as well as a wide variety of aerosol and cloud conditions.

As mentioned earlier, CALIOP validation flights were often flown by HSRL during field missions. Some of these missions were focused solely on CALIOP validation, however most of these missions had multiple objectives. Table 1 summarizes the specific mission information and further demonstrates the large seasonal and spatial sample the HSRL validation flights encompass. The first mission was the CALIPSO-CloudSat Validation EXperiment (CC-VEX), where the HSRL was based out of NASA LaRC in Hampton, VA, and flew primarily along the US Eastern Seaboard. HSRL then participated in several other field studies that included CALIOP validation flights: the Texas Air Quality Study (TexAQS) – Gulf of Mexico Atmospheric Composition and Climate Study (GoMACCS) based out of Houston, TX (Parrish et al., 2009); the Cumulus Humilis Aerosol Processing Study (CHAPS) based out of Ponca City, OK (Berg et al., 2009); the CALIPSO and Twilight Zone (CATZ) field campaign based out of NASA LaRC; a mission dedicated to CALIOP validation flights based in the Caribbean islands; and the Arctic Research of the Composition of the Troposphere from Aircraft and Satellites (ARCTAS) spring and summer deployments based out of Barrow, AK and Yellowknife, NWT, Canada, respectively (Jacob et al., 2010). HSRL also conducted a special series of nighttime flights based out of Hampton, VA, to verify the long-term stability of the CALIOP calibration. These flights covered the period when the CALIOP laser was intentionally transitioned from its primary laser to its backup laser due to a loss of pressure in the primary laser (Hunt et al., 2009) and are discussed further in Sect. 5.3. Most recently, HSRL participated in the Routine ARM Aerial Facility (AAF) Clouds with Low Liquid Water Depths (CLOWD) Optical Radiative Observations (RACORO) campaign based out of Ponca City, OK. In addition, flights not associated with a specific mission were occasionally conducted during transit flights to or from NASA LaRC and other destinations (denoted by "Other" in Table 1 and Fig. 1).

3 Comparison methodology

3.1 CALIOP attenuated backscatter

The CALIOP data products are divided into categories as per the standard NASA Earth Observing System (EOS) nomenclature: level 1 and level 2 (King et al., 2004). The level 1 products are geolocated and calibrated profiles of total attenuated backscatter coefficients at 532 and 1064 nm and the perpendicular polarized component of the total attenuated

Table 1. Summary of HSRL flights and hours along the CALIPSO track for the field missions containing CALIOP validation components.

Mission	Date Range	Number of CALIOP flights	Number of hours on CALIOP track
CC-VEX	14 Jun 2006–7 Aug 2006	11	16.2
TexAQS-GOMACCS	28 Aug 2006–28 Sep 2006	10	13.8
CHAPS	3 Jun 2007–26 Jun 2007	8	10.9
CATZ	19 Jul 2007–11 Aug 2007	4	7.6
Caribbean	24 Jan 2008–3 Feb 2008	7	13.2
ARCTAS (spring)	1 Apr 2008–19 Apr 2008	12	17.5
ARCTAS (summer)	14 Jun 2008–10 Jul 2008	11	10.3
Nighttime Calibration	22 Jan 2009–17 Apr 2009	11	15.9
RACORO	17 Jun 2009–26 Jun 2009	3	4.0
Other	2007–2009	9	6.3
Total		86 flights	115.7 h

backscatter coefficient at 532 nm. Total attenuated backscatter as a function of range, denoted by $\beta'(r)$, is the sum of the parallel and perpendicular components of attenuated backscatter profiles as defined in Eq. (1), denoted with the subscripts $||$ and $\perp$, respectively. This paper deals solely with the 532 nm attenuated backscatter so no wavelength subscript is used on $\beta'(r)$. The attenuated backscatter profile is defined as the product of the backscatter coefficient, $\beta_(r)$, and the two-way attenuation of the atmosphere, $T^2(r)$. This quantity is also written in terms of the measured parallel signal, $P(r)$, range, r, and non-range dependent parameters (the system calibration constant), C:

$$\beta'(r) = \beta'_{||}(r) + \beta'_{\perp}(r)$$
$$\beta'_{||}(r) \equiv \beta_{||}(r)T^2(r) = \frac{P_{||}(r)\Psi(r)}{C_{||}}$$
$$\beta'_{\perp}(r) \equiv \beta_{\perp}(r)T^2(r) = \frac{P_{\perp}(r)\Psi(r)}{C_{\perp}}. \quad (1)$$

The transmitter-to-receiver overlap function is described by $\Psi(r)$; however, all regions examined in this paper were chosen such that this function is not range dependent and it is therefore absorbed into the system constants for subsequent equations. Note that the treatment is identical for the both the parallel and perpendicular polarization components of attenuated backscatter.

The accuracies of the CALIOP level 1 products and many of the level 2 products depend critically on the accuracy of the calibration of the 532 nm parallel component of the attenuated backscatter profiles. First, the level 1 perpendicular polarization signal is calibrated relative to the parallel polarized component of attenuated backscatter. The level 1 total attenuated backscatter, calculated from Eq. (1), is then used to retrieve the level 2 lidar products, which include vertical profiles of aerosol/cloud backscatter and extinction, aerosol/cloud layer base and top heights, and integrated aerosol/cloud layer parameters (e.g., aerosol optical depth). Also, since the 1064 nm signal is calibrated relative to the calibrated 532 nm total attenuated backscatter (Hostetler et al., 2006; Vaughan et al., 2010), the calibration of all data products is fundamentally dependent upon the calibration of the 532 nm parallel signal. The procedure for calibrating the 532 nm parallel component of the attenuated backscatter is described in detail in Powell et al. (2009). Unless otherwise noted, this study uses the version 3.01 dataset (V3.01), released in early 2010.

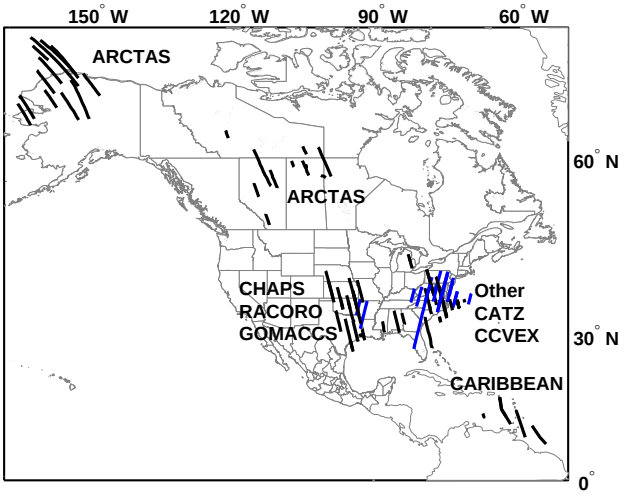

Fig. 1. HSRL flight tracks of CALIPSO underpasses flown from June 2006 through 2010 with approximate mission location noted. Blue flight tracks indicates night time flights.

During nighttime measurements, the CALIOP 532 nm parallel signal is calibrated by determining the ratio between the measured signal (i.e., in digitizer counts) at a set altitude to the total backscatter estimated for that altitude from an atmospheric model (Powell et al., 2009; Hostetler et al., 2006; Russell et al., 1979). The key to accurate calibration is to

choose an altitude for which the atmospheric backscatter can be accurately estimated and the lidar signal has sufficient signal to noise ratio (SNR) and linearity. Solving Eq. (1) for the parallel calibration constant at a given altitude region, r_c gives

$$C_{||} = \frac{r^2 P_{||}(r_c)}{\left(\beta_{||,m}(r_c) + \beta_{||,A}(r_c)\right) T^2(r_c)}. \quad (2)$$

In Eq. (2), the parallel polarization component of the backscatter, $\beta_{||}(r)$, is now expressed as the sum of the molecular, $\beta_{||,m}(r)$, and aerosol, $\beta_{||,A}(r)$, backscatter profiles. The CALIOP 532 nm parallel signal is calibrated by averaging the signal over the 30–34 km range, where aerosol loading is assumed to be low and there is still sufficient molecular backscatter to produce a robust signal (Hostetler et al., 2006; Powell et al., 2009). The current CALIOP calibration algorithm assumes only molecular backscatter in the calibration region, which is computed using molecular number density profiles derived from the NASA Global Modeling and Assimilation Office (GMAO) model (Rienecker, 2008) and a known Cabannes backscatter cross-section (She, 2001; Hostetler et al., 2006). Estimates of the 532 nm parallel channel calibration factor are determined for contiguous 55 km segments of the night side of the CALIOP orbit and are smoothed via a 27-segment (1485 km) running average to reduce noise. The running average calibration value is used to calibrate the nighttime profiles for the level 1 attenuated backscatter products.

For daytime measurements, the high solar background dominates the clear air signal and the subsequent low SNR in the 30–34 km region prevents calibration of the parallel channel via the molecular normalization technique described above. Instead, the daytime signals are calibrated with respect to the calibration established during the previous nighttime orbit. If the magnitudes of the nighttime and daytime signals are uniformly proportional with respect to latitude for a given target (e.g., cloud-free regions between 8 km and 12 km in altitude), then the nighttime calibration coefficient can be readily adapted for daytime conditions via a constant, empirically derived scale factor. This approach was used in the initial release of the CALIOP data, where the daytime calibration was estimated by a linear interpolation of the calibration coefficients at the endpoints of the two nighttime data segments that bracket each daytime data segment. However, it was subsequently shown that this approach led to large errors in the daytime calibration due to thermally driven changes in the alignment between the transmitter and the receiver as the satellite goes through day-night illumination cycles (Powell et al., 2010). These alignment shifts cause the signal levels from identical targets to vary non-linearly over the daytime portion of the orbits and thus preclude the use of a constant scale factor to transfer calibration from nighttime to daytime measurements. To overcome these instrument anomalies, a time-dependent set of scale factors is applied to the nighttime calibration. The scale factors are derived using attenuated scattering ratios calculated over cloud-free regions between 8 km and 12 km in altitude. The goal of this calibration is to produce daytime clean air attenuated scattering ratios that are essentially identical to the nighttime clean air attenuated scattering ratios at the same altitude and latitude. In the version 2 data releases (V2.0x), the scale factors are applied using a five-point piecewise-linear interpolating function (Powell et al., 2008). The version 3 data release improves upon this calibration scheme by applying a 34-point latitudinally-dependent linear interpolating function (Powell et al., 2010). In part because of the challenges experienced with the daytime calibration and the need for external, independent validation of the interpolation function, more HSRL validation flights were conducted during daytime and those flights were conducted over as wide a latitudinal and seasonal range as was practical within the constraints of the B-200 operational parameters and budget.

The calibration of the parallel channel is transferred to the perpendicular channels using data obtained during a polarization calibration operation (Hunt et al., 2009). In this process, a pseudo-polarizer is inserted into the optical path, providing equal signal to both channels and thereby allowing the electro-optical gain between the parallel and perpendicular channels, K_{PGR}, to be determined. The 532 nm perpendicular calibration constant is then written as

$$C_{\perp} = K_{PGR} C_{||}. \quad (3)$$

This paper focuses on the validation of the 532 nm CALIOP calibration by comparison of the total attenuated backscatter ($\beta'_{CALIOP}(r)$), which can be rewritten from Eqs. (1) and (3)

$$\beta'_{CALIOP}(r) = \frac{r^2 P_{||}(r)}{C_{||}} + \frac{r^2 P_{\perp}(r)}{K_{PGR} C_{||}}. \quad (4)$$

Note that the random uncertainty in K_{PGR} is small (<1.0%) and systematic uncertainties are thought to be much smaller than the random uncertainty (Powell et al., 2009).

Previous studies have identified potential biases in the CALIOP attenuated backscatter (Powell et al., 2009; Vernier et al., 2009). Sources of uncertainty in the CALIOP calibration include uncertainties in the model-derived estimate of backscatter in the calibration region, nonlinearity in signal response of the CALIOP detection system, polarization cross talk between the 532 nm parallel and perpendicular channels, and errors from radiation-induced noise spikes. Based on analysis of pre-launch test data and post launch science data, errors due to detector nonlinearity and polarization cross talk are considered to be insignificant (Powell et al., 2009). Radiation-induced spikes in the 532 nm signals (e.g., due to high energy protons impinging on the detector) can affect calibration by causing errors in background subtraction (i.e., subtraction of the digitizer offset and constant background signal from background light) and errors in the signal level measured in the calibration range. These spikes are detected

and eliminated via an adaptive filtering technique (Powell et al., 2009) prior to the calibration process, and therefore should not make a significant contribution to the calibration error.

Uncertainties in the CALIPSO calibration are discussed by Powell et al. (2009) and the CALIOP calibration is expected to have a bias no larger than 5%. This bias attributed to uncertainties in the molecular backscatter in the calibration region (3%), uncertainties in the aerosol backscatter in the calibration region (4%), or unaccounted aerosol, molecular, and ozone transmittance between the instrument and the calibration region (0.5%). The largest uncertainty is due to assumption of negligible aerosol scattering in the calibration region. Indeed, Vernier et al. (2009) estimate that CALIOP level 1 total attenuated backscatter is systematically calibrated low by ∼6% due to unaccounted aerosol scattering up to 35 km in the tropics. Vernier et al. (2009) suggests calibration in the relatively aerosol-free region between 36 km and 39 km identified in both SAGE and CALIOP data, however this is not implemented in CALIOP data processing. This aerosol contribution in the calibration region will be addressed in future versions of the CALIOP calibration algorithm.

3.2 HSRL attenuated backscatter

The airborne HSRL incorporates 532 nm polarization-sensitive elastic backscatter lidar channels similar to those on CALIOP as well as the spectrally-filtered molecular backscatter channel at 532 nm, from which extinction is derived via the HSRL technique. The relative electrical gains and optical attenuations between the channels (the "electro-optic gain ratios") are determined via internal instrument calibrations (Hair et al., 2008). The HSRL 532 nm total attenuated backscatter profiles are determined from the internally calibrated profile measurements in a four-step process. First, the sum of gain-scaled parallel and perpendicular channel signals is divided by the gain-scaled molecular channel signal, yielding the *unattenuated* scattering ratio, $R(r)$, (the attenuation terms in the numerator and denominator cancel in the ratio):

$$R(r) = \frac{P_{||}(r) + \left(\frac{C_{||}}{C_{\perp}}\right)_{\text{est}} P_{\perp}(r)}{\left(\frac{C_{\text{m}}}{C_{||}}\right)_{\text{est}} P_{\text{m}}(r)} = \frac{\beta_{\text{m}}(r) + \beta_{\text{A}}(r)}{\beta_{\text{m}}(r)}. \quad (5)$$

Where Eq. (5) uses the following definitions:

$$\begin{aligned} P_{||}(r) &= \frac{1}{r^2} C_{||} \left[\beta_{\text{m},||}(r) + \beta_{\text{A},||}(r)\right] T^2(r) \\ &= \text{HSRL parallel channel signal} \\ P_{\perp}(r) &= \frac{1}{r^2} C_{\perp} \left[\beta_{m,\perp}(r) + \beta_{A,\perp}(r)\right] T^2(r) \\ &= \text{HSRLperpendicularchannelsignal} \\ P_{\text{m}}(r) &= \frac{1}{r^2} C_{||} \left[\beta_{\text{m},||}(r) + \beta_{\text{m},\perp}(r)\right] T^2(r) \\ &= \text{HSRL molecular channel signal} \end{aligned}$$

$$\begin{aligned} \left(\frac{C_{||}}{C_{\perp}}\right)_{\text{est}} &= \text{parallel-to-perpendicular electro-optic} \\ &\quad \text{gain from internal calibration} \\ \left(\frac{C_{\text{m}}}{C_{||}}\right)_{\text{est}} &= \text{molecular-to-parallel electro-optic gain} \\ &\quad \text{from internal calibration} \end{aligned} \quad (6)$$

Second, this scattering ratio profile ($R(r)$) is multiplied by an estimate of the molecular backscatter profile computed from the GMAO-derived molecular density profile and a Cabannes-only backscatter cross section (Hair et al., 2008), yielding the total (aerosol plus molecular) backscatter profile (in $\text{km}^{-1}\text{sr}^{-1}$):

$$\beta(r) \equiv \beta_{\text{m}}(r) + \beta_{\text{A}}(r) = R(r)\beta_{\text{m,Model}}(r). \quad (7)$$

Note that the HSRL measurement of scattering ratio is related to the unattenuated backscatter profile, $\beta(r)$, and not the attenuated backscatter profile typically measured with an elastic lidar. The 532 nm backscatter profile is then used to calibrate the sum of the HSRL parallel and perpendicular 532 nm channels to produce the 532 nm total attenuated backscatter profile:

$$\beta'_{\text{HSRL}}(r, r_{\text{f}}) = \frac{r^2}{C'(r_{\text{a}}, r_{\text{f}})} \left[P_{||}(r) + \left(\frac{C_{||}}{C_{\perp}}\right)_{\text{est}} P_{\perp}(r) \right], \quad (8)$$

where

$$C'(r_{\text{a}}, r_{\text{f}}) = C_{||} T^2(r_{\text{a}}, r_{\text{f}}) \frac{r_{\text{f}}^2 \left[P_{||}(r_{\text{f}}) + \left(\frac{C_{||}}{C_{\perp}}\right)_{\text{est}} P_{\perp}(r_{\text{f}}) \right]}{R(r_{\text{f}}) \beta_{\text{m,Model}}(r_{\text{f}})} \quad (9)$$

r_{a} = aircraft altitude
r_{f} = altitude to which attenuation is referenced .

For the HSRL profiles, r_{f} is chosen to be the highest altitude region in the profile for which the transmitter-to-receiver optical overlap factor can be considered to be unity. This is typically 1.5 km to 2 km below the aircraft (6.5 km to 7 km altitude). The value of the resulting profile at r_{f} is the total backscatter at that range. For altitudes below r_{f}, $\beta'_{\text{HSRL}}(r, r_{\text{f}})$ is the product of the backscatter and the two-way transmittance from r_{f} to r.

The reference altitude range for CALIOP attenuated backscatter is 30–34 km, a calibration altitude considerably higher than the altitudes measured by the HSRL. The final step in conditioning the HSRL data for assessment of CALIOP calibration is to transfer the reference altitude of the attenuated HSRL backscatter to the CALIOP calibration reference altitude of 30 km. This is done by multiplying the attenuated backscatter profile by an estimate of the attenuation between the r_{f} and 30 km to obtain:

$$\begin{aligned} \beta'_{\text{HSRL}}(r, r_{30\,\text{km}}) &= \beta'_{\text{HSRL}}(r, r_{\text{f}}) T^2(r, r_{30\,\text{km}}) \\ &= \beta'_{\text{HSRL}}(r, r_{\text{f}}) \exp\left[-2 \int_{r_{\text{f}}}^{30\,\text{km}} \alpha(r') dr' \right]. \end{aligned} \quad (10)$$

The transmittance term includes extinction due to molecular scattering and ozone absorption losses estimated from their number densities in the GMAO model between the HSRL 532 nm total attenuated backscatter calibration attitude and that of CALIOP. Background aerosol extinction between the two altitudes is unknown and is therefore not included. However, the presence clouds or thick aerosols above HSRL can lead to large errors in the estimated two-way transmittance, which are further discussed in Sect. 4.2.

In the presence of thin ice clouds Eq. (10) must be modified to include a multiple scattering factor inside of the exponential (Winker, 2003). This factor is not included in the equation because it does not apply to extinction due to molecular scattering or ozone absorption. Also, any aerosol layers above HSRL in this study should be vertically thick (layer thickness >0.5 km) and not require a significant multiple scattering correction (Winker, 2003).

To minimize transmittance errors due to clouds and aerosols, the CALIOP level 2 Vertical Feature Mask (VFM) (Vaughan et al., 2004) is used to detect the presence of clouds and aerosols above the aircraft and eliminate high altitude aerosol or cloud-contaminated profiles from calibration comparisons. Furthermore, a visual inspection of the level 1 attenuated backscatter profiles verified proper VFM identification of high altitude clouds or thick aerosols in the region above HSRL for all cases presented in this paper.

An important aspect of HSRL attenuated backscatter calibration is that it is based on internal instrument calibration. The internal calibration enables accurate estimation of total (i.e., aerosol plus molecular) backscatter, thereby eliminating calibration errors associated with uncertainties in aerosol loading at the calibration altitude. This differs from CALIOP calibration and the calibration of backscatter lidars in general which either (a) assume, sometimes incorrectly, that the aerosol loading in the calibration region is negligible or (b) requires independent information on aerosol loading at the calibration altitude.

3.3 Sample HSRL underflight from 24 September 2006

An example HSRL and CALIOP 532 nm total attenuated backscatter comparison from 24 September 2006 is shown in Figure 2. The time series "curtain plots" of the CALIOP (a) and HSRL (b) 532 nm attenuated backscatter cover a distance of ~270 km along the CALIPSO track indicated in the flight track map (c). The enhanced backscattering in the CALIOP measurements above 13 km on the southern end of the track (less than 34° N) is due to cirrus clouds. As mentioned above, the profiles in which these clouds occur were removed from both the CALIOP and HSRL mean 532 nm total attenuated backscatter profiles (d). These mean profiles are the basis for the difference calculations, calculated by:

$$\text{difference}(r) = 100 \cdot \frac{\bar{\beta}'_{\text{HSRL}}(r, r_{30\,\text{km}}) - \bar{\beta}'_{\text{CALIOP}}(r)}{\bar{\beta}'_{\text{HSRL}}(r, r_{30\,\text{km}})}. \quad (11)$$

Due to the highly variable nature of clouds and thick aerosols in the planetary boundary layer (PBL), the altitude range used in the calculation was restricted to cloud-free regions of the free troposphere, from the aircraft to the top of the PBL, where aerosol loading is generally much lower and much less variable both spatially and temporally. Altitude regions other than the "clear air" free troposphere are addressed on select cases in Sect. 5.4 below.

In this example, the altitude range selected was in the 4–7 km region and yields a mean difference of 2.1% with a standard deviation of 5%. For this case, a less conservative choice on altitude range was not found to create significant differences. For instance, using altitude range of 1–7 km yields similar results (average difference = 2.7% ± 5%). However, the conservative approach of staying well above the PBL is followed for the calibration assessment results presented in this paper.

4 Uncertainty due to the comparison methodology

Systematic and random uncertainties due to the HSRL validation methodology must be discussed to truly assess the CALIOP calibration. This ensures the reported differences of CALIOP 532 nm total attenuated backscatter relative to that of HSRL are only due to the CALIOP calibration scheme, and not due to the calculation of HSRL attenuated backscatter or the scaling of the HSRL data to the CALIOP calibration region discussed in Sect. 3.2. Differences due to temporal mismatch of the HSRL and CALIOP measurements should average to zero given the large number of cases; however this is also verified.

4.1 Uncertainty due to the HSRL calibration of attenuated backscatter

Systematic differences between HSRL and CALIOP 532 nm total attenuated backscatter profiles could be due to a bias in the HSRL calibration of attenuated backscatter (aerosol or molecular backscatter in the 7 km calibration region and the transmittance to the calibration region), or the scaling of HSRL attenuated backscatter to the CALIOP calibration altitude (30–34 km).

Similar to CALIOP, HSRL derives an estimate of molecular backscatter using the GMAO meteorological model to infer molecular number density and an estimate of the Cabannes cross section (Hair et al., 2008). The Cabannes backscatter cross section is a straightforward theoretical calculation (She, 2001) and the value used by HSRL is consistent with that of CALIOP (within 0.09%). Any uncertainty in the molecular backscatter will be dominated by the accuracy of the GMAO model which is used by both CALIOP and HSRL in the data retrievals. Hair et al. (2008) estimated the error due to temperature and pressure in the HSRL molecular backscatter to be less than ±1%.

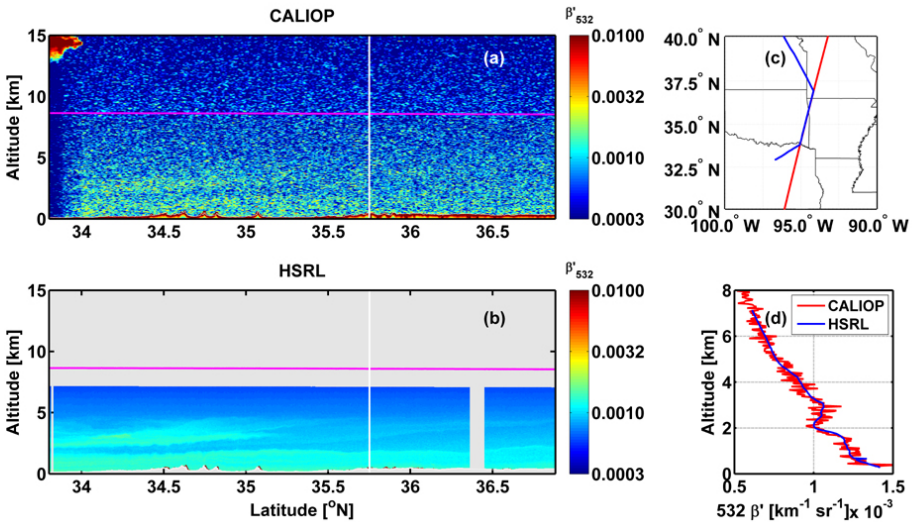

Fig. 2. The 532 nm attenuated backscatter curtains referenced to 30 km from **(a)** CALIOP (5 pt temporal running average) and **(b)** HSRL on 24 September 2006 from 08:00 to 09:15 UTC. The white vertical line indicates the closest point of approach (CPA), 08:20 UTC, and the magenta horizontal line indicates the B-200 flight altitude. The flight track map **(c)** shows the HSRL flight path (blue) and CALIOP (red). Mean HSRL (blue) and CALIOP (red) 532 nm total attenuated backscatter profiles are shown in **(d)**.

Unlike standard backscatter lidars, the HSRL technique implemented does not rely on a calibration from the atmosphere. The internal calibration of the airborne HSRL has been thoroughly examined and uncertainty in the aerosol backscatter profiles is estimated to be less than ±2.3% (Hair et al., 2008).

Atmospheric attenuation between the HSRL (aircraft) altitude and the HSRL attenuated backscatter calibration region is due to aerosol and molecular extinction as well as ozone absorption (Eq. 9). The HSRL calculation of attenuated backscatter only accounts for the molecular scattering. This is accomplished using the GMAO model and an estimate of the Rayleigh scattering coefficient, which amounts to approximately an attenuation of 1.6% for nominal HSRL altitudes. Note that the molecular attenuation was not accounted for in Powell et al. (2009), so the resulting biases presented there are larger than those reported here. The ozone absorption is not accounted for in the HSRL calculation of attenuated backscatter because the ozone absorption is estimated to be approximately 0.05% for nominal HSRL altitudes. While HSRL measures the aerosol scattering ratio in this region, the aerosol extinction (and hence aerosol transmittance) is not calculated due to system overlap. The aerosol transmittance is therefore neglected in Eq. (9); however observing large scattering ratios in this region can be used to quality assure the HSRL attenuated backscatter. To estimate the maximum bias due to the neglected aerosol attenuation, the aerosol extinction is integrated assuming a scattering ratio of 1.05 (Eq. 5) and a lidar ratio of 50 sr. This amounts to a conservative estimate of less than ∼0.5% uncertainty due to unaccounted aerosol transmittance.

4.2 Uncertainty due to the estimate of the two-way transmittance used to scale airborne HSRL attenuated backscatter to the CALIOP reference altitude (30–34 km)

The two-way molecular scattering and ozone absorption leads to attenuation between the HSRL attenuated backscatter calibration altitude (∼7 km) and the CALIOP calibration altitude (30 km). The transmittance in this study is typically around 87% (Eq. 10, $T^2_{\text{molecular+ozone}}$). Potential biases which could influence the transmittance term can be due to ozone absorption, molecular scattering, and clouds or aerosol attenuation. Because the aerosol and cloud profiles are unknown, they are not accounted for in the transmittance term; only the transmittance from molecular scattering and ozone absorption is included. Uncertainty in the molecular scattering (due to accuracy of the GMAO temperature profile) is thought to be less than ±2% (Russell et al., 1982), based on the altitude range considered (0–30 km). The ozone attenuation term is small (T^2_{ozone}) so any bias induced by this correction should be negligible.

The CALIOP VFM is used to remove any profiles with cloud, aerosol, or stratospheric layers above the HSRL measurements; however undetected features will introduce biases into the comparisons. To bound the maximum potential bias introduced by undetected high altitude aerosols and clouds, the CALIOP level 2 (layer product, version 3.01, 5 km resolution product) cloud optical thicknesses (COT) were computed above the HSRL altitude for all 86 flight tracks (Fig. 3). The minimum CALIOP COT above HSRL provides an estimate of the minimum detectable COT and the maximum bias introduced by undetected clouds. Although the HSRL

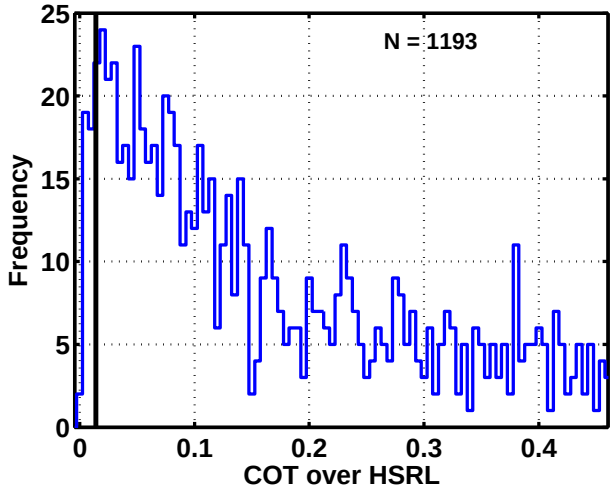

Fig. 3. Histogram of cloud optical thicknesses for clouds above 7.5 km and consequently above the maximum height observed by HSRL from all flights (day and night). The vertical black line corresponds to a COT of 0.0125.

validation flights generally targeted cirrus free forecasts, a significant amount of COT over a portion of the HSRL track is observed on approximately 25% of the flights. The minimum COT found in this dataset was 0.0016, but we estimate an upper bound of the minimum COT of 0.0125 from Fig. 3 (slightly less than the most frequent COT). The COT reported by CALIOP is the single scattering COT (i.e. corrected for multiple scattering) (Winker, 2003). As mentioned in Sect. 3.2, the CALIOP level 1 product comparison presented here would be biased by the transmittance due to both single and multiple scattering, so the minimum COT is multiplied by a multiple scattering factor of 0.6, which applies for ice clouds only (Winker, 2003). This results in a minimum detectable COT of 0.0075, or a maximum bias due to undetected clouds of 1.5%. Due to the large number of daytime flights relative to nighttime considered in Fig. 3, the bias is more representative of daytime detection values. This analysis is consistent with an expected daytime bias value estimated from CPL measurements. McGill et al. (2007) determined that the CALIOP minimum detectable backscatter (MDB) at 5 km resolution is approximately 1.7×10^{-3} km^{-1} sr^{-1} (daytime). Scaling this value to 80 km (multiply by sqrt(80/5)) to compare with the above analysis, we estimate the 80 km MDB to be approximately 4.25×10^{-3} km^{-1} sr^{-1}. Now, assuming a mean lidar ratio of 25 sr (Winker et al., 2009) (multiply by 25 sr) and layer thickness of 1 km (multiply by 1 km), the minimum detectable optical thickness is estimated to be 0.0106. Accounting for the two way transmittance (multiply by 2) and ice cloud multiple scattering factor (multiply by 0.6), the bias due to undetected clouds is approximately 1.3% ($T^2_{\text{cloud}} = 0.987$), agreeing with the above analysis. In summary, thin clouds not detected by the CALIOP L2 VFM used for cloud screening may introduce a bias no larger than 1.5%. Unlike the molecular uncertainty discussed above, cloud contamination between HSRL and CALIOP will systematically affect the comparison, introducing a bias.

Neglecting undetected aerosols may also bias the transmittance term. However, the optical depth in the upper troposphere and stratosphere is generally low (AOD < 0.005) in the absence of any large injections of aerosol into the stratosphere (Jäger, 2005). In a relevant example, Rogers et al. (2009) found the 532 nm AOD above 6.3 km to be 0.01 during the Megacity Initiative: Local and Global Research Observations (MILAGRO) campaign during 2006 in Mexico. In order to estimate the possible bias introduced by unaccounted aerosol transmittance, a constant scattering ratio of 1.05 and a lidar ratio of 50 sr is assumed in the 30 km to 8 km region and yields a maximum undetected AOD of 0.011 ($T^2_{\text{aerosol}} = 0.978$). On occasion, volcanic activity can inject plumes into the upper troposphere and lower stratospheric region with large scattering ratios and 532 nm optical depths exceeding 0.025 (Mattis et al., 2010). In general volcanic plumes are not always identified in the CALOP VFM, although the temporal average in this study should allow the thicker volcanic layers to be identified by manual inspection of the profiles. From Mattis et al. (2010), we estimate the maximum upper troposphere plus stratospheric optical depth to be around 0.015, with a careful examination of the data recommended closer than one month to volcanic activity. This corresponds to a maximum bias of 3.0% due to unaccounted aerosol attenuation.

4.3 Temporal mismatch between the airborne HSRL and CALIOP observations

The HSRL and CALIOP mean 532 nm attenuated backscatter profiles in the previous sections were averaged in time over the entire (cloud-free) spatially coincident HSRL flight track to ensure the best SNR in the CALIOP profile. However, the actual HSRL and CALIOP coincidence occurred instantaneously, at a single location and time during each flight. Generally, the free troposphere "clean air" is spatially and temporally stable for the time and space scale considered in this study (Anderson et al., 2003). The stability is tested by evaluating the clean air difference as a function of time from the closest point of approach (CPA) (i.e., where the aircraft and satellite are coincident in time). This is accomplished by averaging the HSRL 532 nm total attenuated backscatter into 20 min bins centered about the CPA. The spatially corresponding CALIOP data were similarly averaged and the mean differences calculated as functions from the CPA. Because each flight has a different mean difference and this hypothesis investigates relative changes, the mean difference for the entire flight is subtracted from each 20 min bin for each flight.

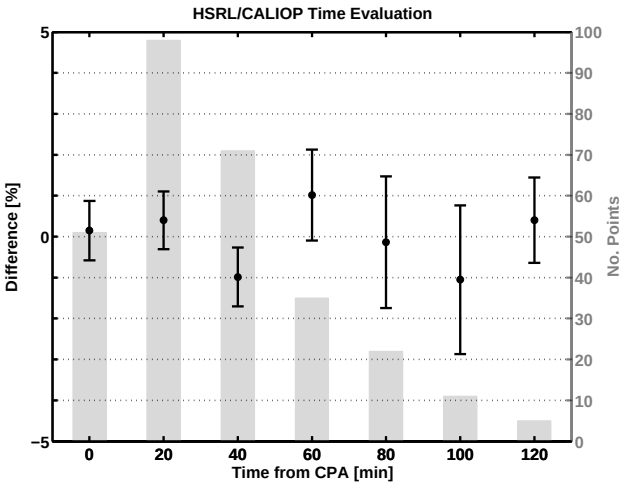

Fig. 4. The relative difference as a function of time from the CPA. Relative differences were binned into 20 min bins with the mean and standard deviation of each bin reported (black) and the number of points in each bin (grey bars).

Figure 4 summarizes the relative differences for all flights, with the mean and standard deviation of the relative differences plotted for each 20 min bin as well as the number of points in each bin (grey bars). No significant discrepancies (within 1%) are observed as the time from the CPA is increased. This indicates that the mean difference for each flight is a good approximation for the mean difference at the CPA and the temporal averaging of the entire profiles does not influence the analysis.

4.4 Summary of systematic biases and uncertainties

All known potential systematic and random uncertainties in the validation methodology are presented to ensure any reported differences of the CALIOP 532 nm total attenuated backscatter relative to HSRL are solely due to the CALIOP calibration scheme. Systematic differences could be introduced by uncertainty in the HSRL calibration of attenuated backscatter (aerosol or molecular backscatter in the 7 km calibration region and the transmittance to the calibration region), or the scaling of HSRL attenuated backscatter to the CALIOP calibration altitude (30 km). The temporal mismatch between HSRL and CALIOP was not found to introduce any uncertainty.

All of the uncertainties are summarized in Table 2. The dominant error source is due to the scaling of the HSRL 532 nm total attenuated backscatter from the HSRL calibration altitude (7.5 km) to that of CALIOP (30 km). As mentioned above, the biases with a known sign (e.g. cloud or aerosol contamination between HSRL and CALIOP will cause a positive bias) are distinguished from the uncertainties, which will not bias the comparison consistently in a single direction. At most the biases can lead to a maximum possible difference of 4.5% (CALIOP lower) with the uncertainties amounting to a maximum of $\pm 3.2\%$ (in a root sum square (RSS) sense). Because these potential error sources are not known, they are not corrected for in this paper. The intent of Table 2 is to rigorously establish the maximum uncertainty from all sources that must be considered for CALIOP validation with an airborne lidar.

5 Results

5.1 Version 3.01 CALIOP 532 nm total attenuated backscatter comparison with HSRL

As discussed in Sect. 3.3, relative difference profiles are calculated in the clean air region from the mean HSRL and CALIOP 532 nm total attenuated backscatter profiles for each flight. The large number of coincident measurements allows a statistical comparison to be performed. The resulting differences in the clean air regions identified for all 86 flights are summarized in Fig. 5. Due to differences in the CALIOP calibration approach for the day and night segments of the orbit, the calibration differences in Fig. 5 are plotted separately based on lighting conditions.

The nighttime difference distribution is a direct assessment of the CALIOP 532 nm total attenuated backscatter calibration procedure and shows a mean difference of +2.7% with a standard deviation of 6.3%. The daytime difference is slightly larger, with a mean difference of +2.9%, and standard deviation of 20%. The larger spread of the daytime distribution is due to noise in the solar background. Indeed, we found that the amount of daytime spread relative to the nighttime agrees well with the calculated random error due the background signal of CALIPSO for these flights, calculated following Liu et al. (2006).

In order to assess the latitudinal and seasonal dependence of the version 3.01 dataset, the mean difference profiles were averaged vertically and horizontally over cloud-free regions of the free troposphere to obtain a single difference point for each HSRL underflight and assigned the mean latitude for that underflight. The difference from each flight is shown in Fig. 6 as a function of latitude and colored by month, similar to results shown in Fig. 11 of Powell et al. (2009). In this analysis, each vertical sample was treated as an independent measurement so the error bars represent the standard error of the mean (i.e. the standard deviation divided by the square root of the number of points).

As expected from Fig. 5, the mean difference of each flight is generally positive in both day and night lighting conditions. The means of these data points are also positive (2.7% nighttime and 2.9% daytime, CALIOP lower), with the standard deviations (2.1% nighttime and 3.9% daytime), representing the measured variability of the average calibration difference.

Table 2. Summary of systematic and random uncertainty sources that may influence the validation of the CALIOP 532 nm total attenuated backscatter with the airborne HSRL measurements.

Uncertainty in the HSRL calculation of attenuated backscatter	
HSRL Molecular Backscatter	±1%
HSRL Aerosol Backscatter	±2.3%
Transmittance to calibration region	±0.5%
Uncertainty in scaling the HSRL attenuated backscatter to 30 km	
Molecular Scattering	±2%
Ozone Absorption	∼0%
Aerosol Scattering	0–3%
Cloud Extinction	0–1.5%
Maximum Uncertainty	4.5%±3.2%

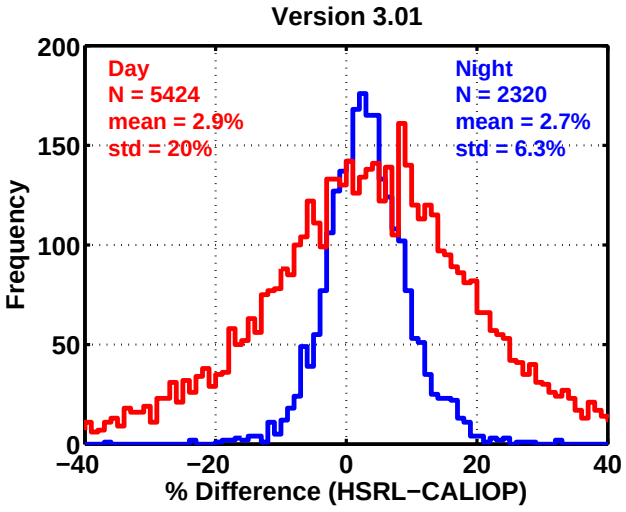

Fig. 5. Distribution of the average 532 nm attenuated backscatter difference in the clear air regions identified for all night (blue) and day (red) flight.

The nighttime flights show a slight seasonal dependence, with higher differences seen in the summertime (June and August) months and lower differences in the spring/winter months. These differences are most likely due to stratospheric aerosol in the CALIOP calibration region in the summertime months for these latitudes (Hostetler et al., 2006) or aerosol loading in the free troposphere (Vernier et al., 2010), and are discussed further in Sect. 3. The daytime differences do not have an obvious latitudinal or seasonal dependence, expected due to improvements in the CALIOP version 3.01 daytime calibration via the interpolation function. Many of the outliers are from flights where only a short segment of the flight track was considered (e.g. screened due to cirrus above the aircraft). The smaller horizontal averaging of CALIOP data for these cases results in larger error bars.

5.2 Version 2.0x CALIOP 532 nm total attenuated backscatter comparison with HSRL

The version 3.01 CALIOP level 1 product was released in early 2010, with significant modifications made to improve the overall operational code; the modification to the version 3.01 daytime calibration algorithm was discussed in Sect. 3.1. An example of the improvement from the version 2.0x to the version 3.01 CALIOP 532 nm total attenuated backscatter daytime measurements was observed by HSRL on 16 October 2008 (Fig. 7). The version 2.0x clean air difference was 20.2% and the version 3.01 difference was 1.9% for this example, which is by far the largest difference observed in the version 2.0x data product.

The version 2.0x clean air differences for all HSRL flights are summarized in Fig. 6c and d. The mean nighttime difference for version 2.0x is nearly identical (2.2%) to that of version 3.01, which is expected because the CALIOP nighttime calibration procedures were essentially unchanged in version 3.01. The version 2.0x daytime difference (1.3%) was slightly smaller than the difference observed in version 3.01; however this is due to more negative differences in the version 2.0x comparison. Indeed, the standard deviation of the version 2.0x comparison is 5.1% in the daytime, which is larger than in corresponding standard deviation in the version 3.01 comparison (3.9%). Overall, many of the version 2.0x daytime flights with differences larger (smaller) than 10% (−10%) in Fig. 6 show significant improvement in the CALIOP version 3.01 calibration, such as the 16 October 2008 case highlighted in Fig. 7.

5.3 CALIOP 532 nm attenuated backscatter calibration through the 2009 laser switch

The CALIOP primary laser was intentionally shut down in February 2009 due to a slow loss of pressure in the primary laser canister and CALIOP switched to the backup laser (Hunt et al., 2009). A dedicated series of nighttime

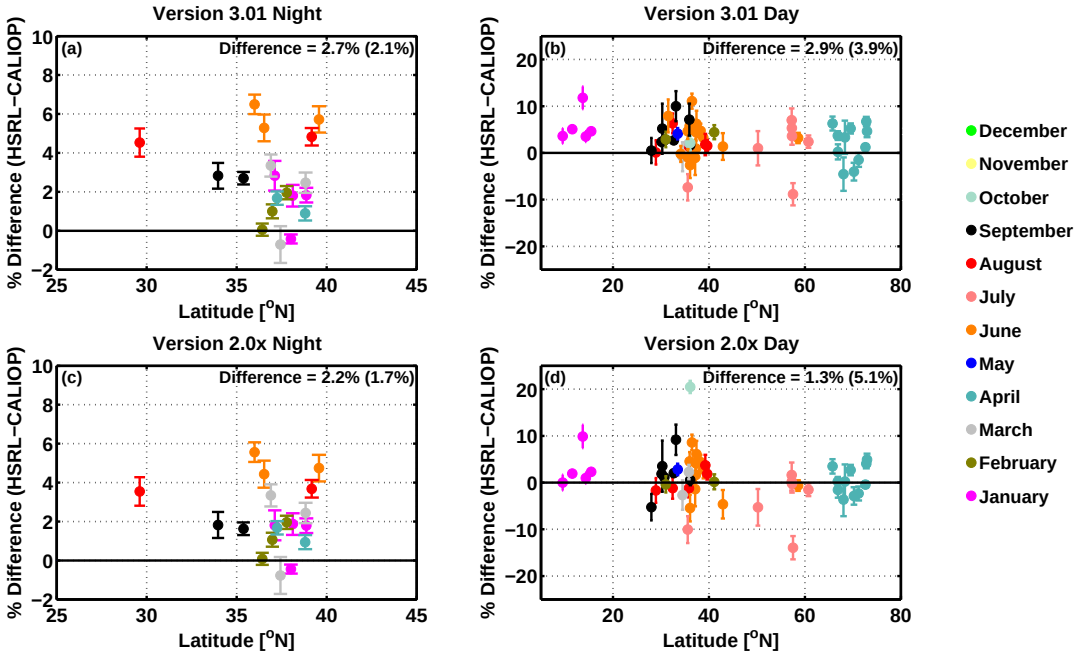

Fig. 6. Version 3.01 532 nm total attenuated backscatter differences for **(a)** night and **(b)** daytime lighting conditions as functions of latitude and month (color). Each data point represents the average clean air difference over an entire HSRL flight. Version 2.0x differences (discussed in Sect. 5.2 below) are also shown for night **(c)** and day **(d)**.

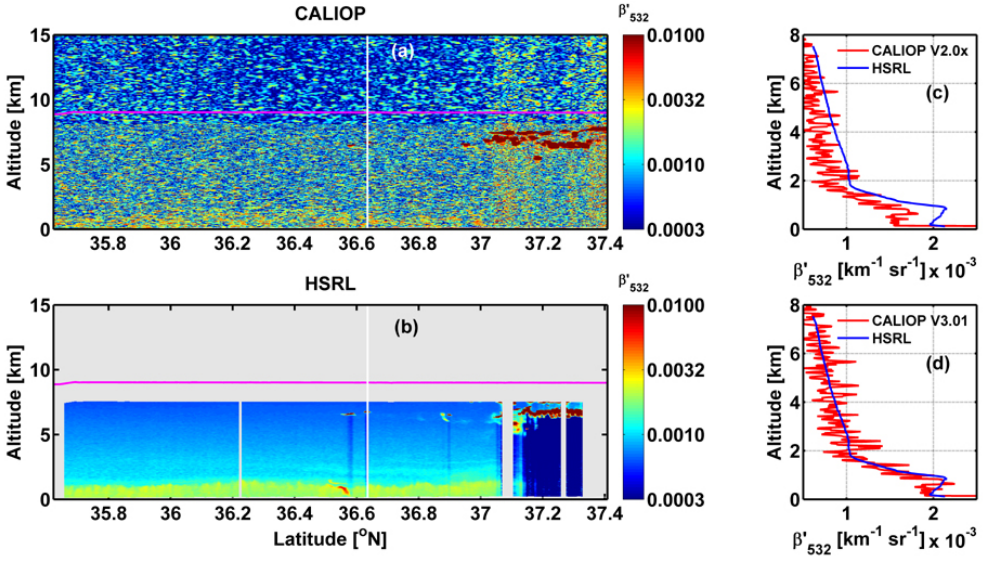

Fig. 7. Time series (**a** and **b**) same as Fig. 2 except for daytime flight on 16 October 2008 over North Carolina and Virginia. Average 532 nm total attenuated backscatter profiles (cloud screened) for CALIOP version 2.0x and version 3.01 are also shown compared to HSRL (**c** and **d**).

HSRL validation flights was performed to ensure calibration consistency across the laser transition, with six flights prior to the laser switch and five follow up flights to assess the backup laser. Figure 8 shows the flight tracks and differences from these dedicated flights. The differences are nearly identical for the primary laser (0.91%) and the backup laser (1.2%) and indicate that the CALIOP 532 nm total attenuated backscatter calibration was maintained through the laser switch.

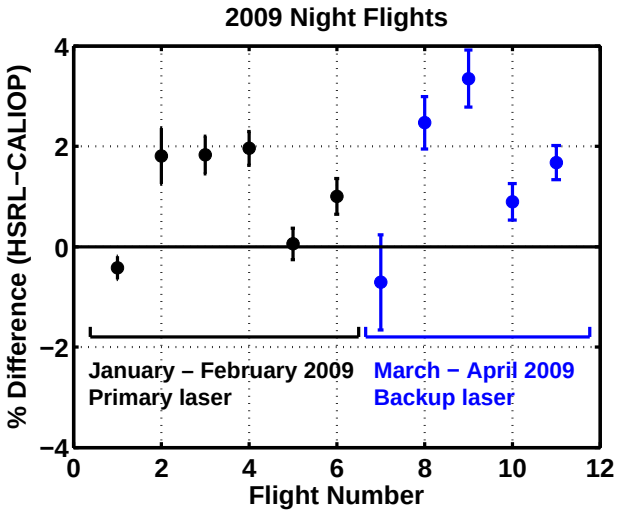

Fig. 8. Flight track map showing the locations of the HSRL underflights of CALIPSO between January and April 2009 **(a)** and the corresponding 532 nm attenuated backscatter differences **(b)**. Night flights show the consistent calibration of CALIOP primary (black) and backup (blue) laser.

5.4 Altitude dependence of the CALIOP 532 nm total attenuated backscatter?

To assess whether the CALIOP 532 nm total attenuated backscatter has any altitude dependence with respect to that of HSRL, difference profiles were computed as a function of altitude over the full vertical range of the HSRL profiles. While Anderson et al. (2003) indicate that there should be little expected variation in aerosol concentration within a few hours on average, the largest variations are expected to occur inside the PBL (rather than in the free troposphere) due to local sources of aerosol, higher relative humidity, changing meteorological conditions, and other similar factors. In order to examine the temporal variability further, the HSRL attenuated backscatter profiles were examined on flights that flew a CALIPSO track and then back tracked the same path on the return to base. The overlapping tracks were matched up in a gridded latitude/longitude space, allowing a direct measurement of how much the attenuated backscatter profile changed as a function of time (at multiple matching locations along the track). This analysis suggested that the HSRL attenuated backscatters were well correlated ($r^2 > 0.9$) in the PBL with up to at least 45 min separation.

Therefore, a subset of the 86 flight comparison dataset was considered with tighter constraints on temporal separation of HSRL and CALIOP. In this subset, only HSRL data within 45 min of the CALIOP closest point of approach were considered, which is slightly larger than the 30 min criterion used by Mona et al. (2009). Furthermore, because clouds are highly variable in the atmosphere both HSRL and CALIOP data were screened for clouds at all altitudes using both the CALIOP VFM and HSRL cloud detection routine (detected as sharp gradients in the raw signals using a three point Haar wavelet covariance transform, Gamage and Hagelberg, 1993), as well as a manual inspection to ensure that only cloud-free profiles were used in the comparison. A total of twenty two cases (eight nighttime and fourteen daytime) was found to meet all of these selection criteria. The HSRL and CALIOP mean 532 nm total attenuated backscatter profiles for all twenty two cases are presented in Fig. 9.

The mean difference profile from all twenty two flights is shown in Fig. 10, separated by day and night. For plotting purposes, the differences were binned into 500 m bins, with the error bars representing the standard error of the mean for each bin. Further averaging the day and night profiles together, a near-constant difference of 3.1% is observed throughout the profile, which is consistent with the "clear air" difference of these twenty two flights (2.4%). To estimate the change over altitude, a linear regression was performed treating the altitude as the independent variable allowing the percent difference to be expressed as:

$$\text{difference}\,[\%] = 0.011 \cdot \text{altitude}\,[\text{km}] + 3.1\%. \quad (12)$$

The slope of 0.011% per kilometer suggests that over a 10 km range the difference will vary by less than 0.1% due to vertical variability and the vertical range selected for each flight does not influence the results in cloud-free regions.

Figure 11 shows the mean CALIOP 532 nm total attenuated backscatter plotted against that of HSRL for all altitudes of all twenty two cases. Clearly, they are well correlated ($r^2 = 0.88$) and have a slope near unity (slope = 1.03) across a large range of attenuated backscatter values. This demonstrates the consistent accuracy of the CALIOP attenuated backscatter over the large dynamic range of aerosol loading present in these twenty two cases. Note that the lowest attenuated backscatter reported by HSRL ($\sim 0.6 \times 10^{-3}\,\text{km}^{-1}\,\text{sr}^{-1}$) is limited by molecular scattering at the highest altitude that HSRL calculates attenuated backscatter.

6 Discussion and conclusions

The results and methodology of the most extensive systematic study of the CALIPSO 532 nm total attenuated backscatter product to date are presented using an internally calibrated airborne HSRL, providing an independent verification of the CALIOP calibration. The version 3.01 CALIOP 532 nm total attenuated backscatter was found on average to be only slightly lower ($2.7\% \pm 2.1\%$) that the HSRL 532 nm attenuated backscatter in clean air during nighttime measurements, directly validating the CALIOP calibration algorithm. A slight seasonal dependence is observed in the nighttime differences, which is attributed to the stratospheric aerosol influence on the CALIOP calibration in the summertime months for the latitudes of nighttime HSRL operation.

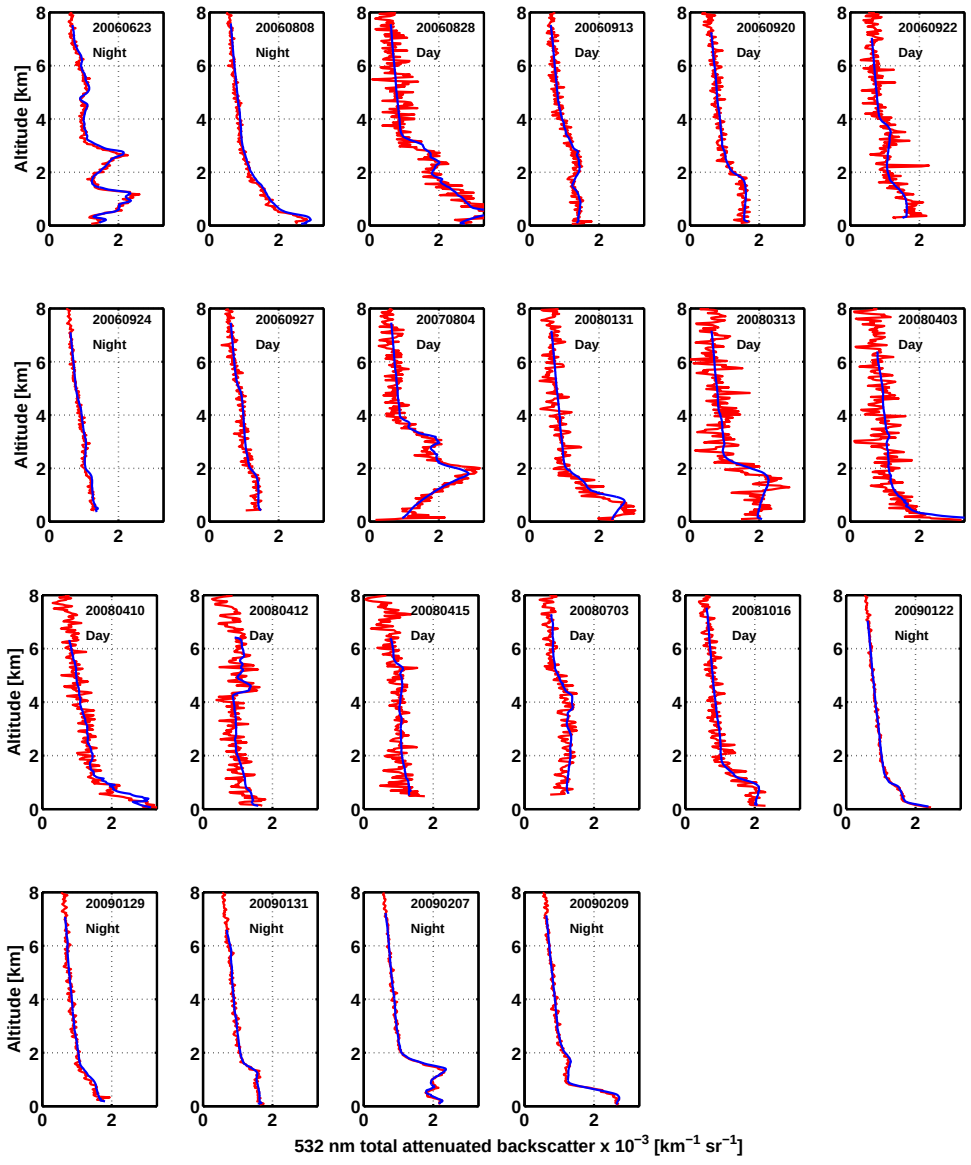

Fig. 9. Mean CALIOP (red) and HSRL (blue) 532 nm attenuated backscatter for all 22 cases meeting the criterion in the text for an assessment of the complete CALIOP vertical profile.

Additionally, this study also found no change in the nighttime calibration of 532 nm total attenuated backscatter through the laser change out in early 2009. This study also quantitatively assesses the daytime version 3.01 CALIOP 532 nm total attenuated backscatter coefficients, which are found on average to be only slightly lower ($2.9\% \pm 3.9\%$) than the HSRL 532 nm attenuated backscatter measurements. Furthermore, the daytime calibration values exhibited no obvious latitudinal or seasonal dependence (within $\sim$10%), indicating accurate performance of the version 3.01 daytime interpolation function.

The comparison methodology presented here is thoroughly examined and intended to establish a model for satellite lidar validation with an airborne lidar. Systematic and random uncertainties considered in this methodology include the following: HSRL calibration of attenuated backscatter due to errors in the aerosol and molecular backscatter in the calibration region and transmittance to the HSRL calibration region; biases due to scaling the HSRL attenuated backscatter to the CALIOP calibration region; biases due temporal and spatial offsets of the HSRL and CALIOP measurements. The error derived from the analysis presented here is smaller than $4.5\% \pm 3.2\%$ (CALIOP lower). This implies that the CALIOP 532 nm total attenuated backscatter profiles are well calibrated within the ability of HSRL to measure.

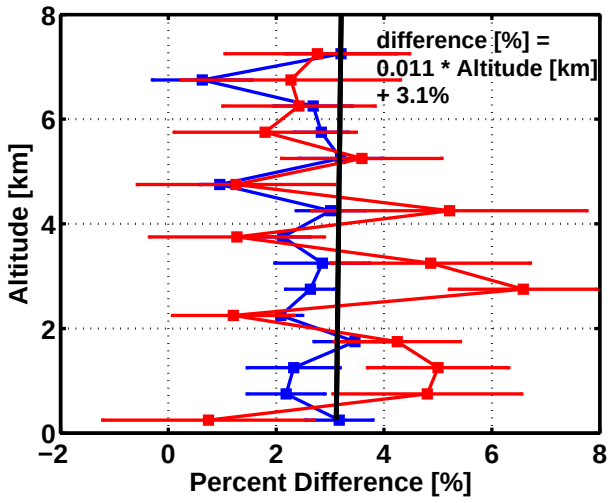

Fig. 10. The mean difference between HSRL and CALIOP for all 22 cases presented in Fig. 9, separated by day (red) and night (blue). The black line represents the linear regression of all 22 cases (treating altitude as the dependent variable).

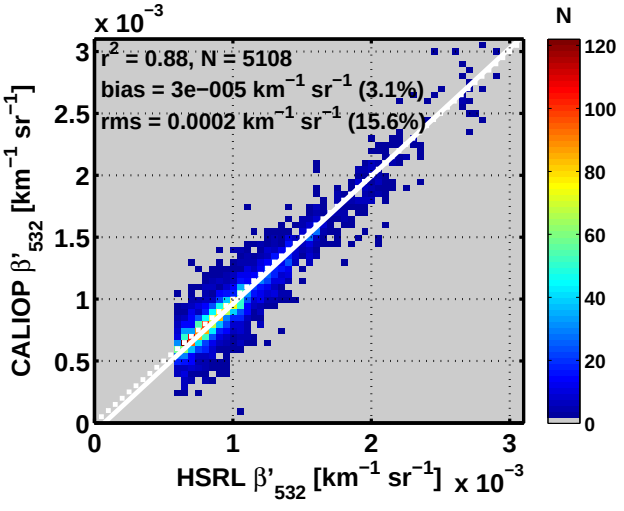

Fig. 11. Scatterplot of HSRL and CALIOP 532 nm total attenuated backscatter values from the 22 cases presented in Fig. 9. The white dotted line indicates the one to one line and the solid white line is a bilinear fit. The colorbar indicates the number of points in each bin.

In addition to aircraft studies previously discussed (McGill et al., 2007), ground based lidars have also offered an assessment of CALIOP attenuated backscatter profiles. Kim et al. (2008) qualitatively show good agreement between an elastic backscatter lidar and CALIOP attenuated backscatter. In another study, Mamouri et al., 2009 used a ground based Raman lidar for nighttime validation and an elastic backscatter lidar for daytime validation of the CALIOP 532 nm total attenuated backscatter. Note that a Raman lidar has an advantage for validation over an elastic backscatter lidar because the Raman lidar technique, like the HSRL technique, provides a more direct measurement of the extinction profile. However, comparisons of nadir (CALIOP) and zenith (ground-based) lidar profiles can have higher uncertainties due to differences in viewing geometry. For example, Ansmann (2006) found that Klett retrievals from zenith-viewing lidar could differ in extinction and backscatter profiles by as much as 20% from a nadir-viewing lidar observing the same scene due to the viewing geometry in complex scenes (e.g. multilayered), with better agreement in simple schemes (e.g. single lofted aerosol plume).

Two ground based Raman lidar studies have provided quantitative assessment of the CALIOP 532 nm attenuated backscatter calibration and show promising results. In clear sky conditions, Mona et al. (2009), found CALIOP to bias slightly low in the free troposphere and very low in the PBL (below 2.5 km). Pappalardo et al. (2010) show similar results from comparisons between several EARLINET lidars and CALIOP with similar results. Additionally, Powell et al. (2009) present the first nighttime HSRL validation flights through 2008, which are a subset of data presented here. However, the results from Powell et al. (2009) did not account for molecular transmittance in the HSRL calibration (see Sect. 4.1) which resulted in an overestimation in HSRL by approximately 1.6%. Table 3 summarizes the published lidar studies which quantitatively assess CALIOP level 1 attenuated backscatter to date.

The differences found in this study agree in the free troposphere with the results from previous studies. However, this study found good agreement between HSRL and CALIOP 532 nm total attenuated backscatter inside the PBL (below ∼3 km) while previous studies suggest that CALIOP may be biased low in this region. In Sect. 5.4 the vertical profile analysis clearly demonstrates that the CALIOP attenuated backscatter profiles are linear through the vertical range investigated and the assessment in the free troposphere applies to the entire vertical profile. Note that these previous quantitative studies were conducted using ground based lidars. Due to differences in the nadir (CALIOP) versus zenith (ground-based) viewing geometries and spatial mismatch, such comparisons may lead to ambiguous results. Discrepancies between nadir- and zenith-viewing approaches may be due to spatial offset of the ground station and the CALIPSO track or temporal averaging of the CALIOP data around the overpass, coupled with influences of local sources and complex terrain between the satellite track and the ground station (Mona et al., 2009). The largest discrepancies due to these considerations are expected appear in the PBL. Indeed, consider the average minimum distance presented by Mona et al. (2009) was 66.5 km. Assuming a uniform 20 km/h wind (also assuming directly between the CALIPSO track and the lidar), the minimum equivalent temporal separation between the measurements is over 3 h, when the aerosol correlation starts to decrease (Anderson et al., 2003). Another potential error source is the estimation of a nadir viewing attenuated

Table 3. Summary of lidar studies to date quantitatively validating the CALIOP level 1 532 total attenuated backscatter product. Note that all differences are reported in terms of "Lidar – CALIOP" and that all previous studies used the CALIOP version 2 data release.

Study	Number of cirrus free cases	532 nm attenuated backscatter difference [%]	Altitude range
Pappalardo et al. (2010)	46, night	$4.6\% \pm 50\%$	1–10 km
Mona et al. (2009)	11, night	$24\pm 20\%$	< 2.5 km
		$2 \pm 12\%$	3–8 km
Mamouri et al. (2009)	12, day	$10\pm12\%$	3–10 km
	15, night	$34\pm34\%$	1–3 km
		$4\pm6\%$	3–10 km
		$15\pm16\%$	1–3 km
Powell et al. (2009)	9, night	5%	$\sim$ 3 km–7 km[a]
This study (version 2.0x)	56, day	$1.3 \pm 5.1\%$	$\sim$ 3 km–7 km[a]
	20, night	$2.2 \pm 1.7\%$	
This study (version 3.01)	66, day	$2.9 \pm 3.9\%$	$\sim$ 3 km–7 km[a]
	20, night	$2.7 \pm 2.1\%$	

[a] Altitude ranges varied, but no dependence noted.

backscatter profile from a zenith viewing lidar (Pappalardo et al., 2010), with potential errors at the lower altitudes due to inaccuracies in the lidar overlap function (Wandinger and Ansmann, 2002). We stress that the airborne HSRL measurements presented here are in agreement with previous (ground based) studies in the free troposphere where ground based overlap and local aerosol influences are less of an issue than in the PBL. We therefore conclude that the there is no altitude dependence of the calibration.

This study further expands the scope of previous validation efforts by including both night and day comparisons that cover a wide range of latitudes, thus greatly increasing the number of validation cases of CALIOP 532 nm attenuated backscatter with considerably smaller systematic uncertainties. Finally, this study takes advantage of the recent release of the CALIOP version 3.01 data, and provides validation of both version 2.0x and version 3.01 products. The comparison between HSRL and CALIOP 532 nm total attenuated backscatter were similar in mean difference and standard deviation for the nighttime version 2.0x and version 3.01 comparisons. However, the daytime CALIOP version 3.01 product differences shows smaller standard deviation than the version 2.0x comparison, hence a better interpolation scheme.

The HSRL has acquired a substantial CALIOP validation dataset over a large temporal and spatial range. Nadir-viewing observations made along the CALIPSO ground track via the self-calibrated HSRL technique provide, to our knowledge, the best means by which to assess CALIOP calibration accuracy and the level products. This rich dataset will be used in the future to continue to assess the CALIOP level 1 532 nm and 1064 nm products as well as the level 2 products, which will be the subject of a future study.

Acknowledgements. We gratefully acknowledge the NASA LaRC Research Service Directorate for their support of B-200 flight operations and the CALIPSO team and data center for CALIOP data production and access. Support for the HSRL deployments and the analyses of these data was provided by the NASA Science Mission Directorate, the NASA CALIPSO project, and the Office of Science (BER), US Department of Energy (Atmospheric Science Program, now Atmospheric System Research Program), Interagency Agreement No. DE-AI02-05ER6398. We also thank the paper reviewers for their helpful comments.

Edited by: G. Vaughan

References

Anderson, T. L., Masonis, S. J., Covert, D. S., Ahlquist, N. C., Howell, S. G., Clarke, A. D., and McNaughton, C. S.: Variability of aerosol optical properties derived from in situ aircraft measurements during ACE-Asia, J. Geophys. Res., 108, 8647, doi:10.1029/2002JD003247, 2003.

Ansmann, A: Ground-truth aerosol lidar observations: can the Klett solutions obtained from ground and space be equal for the same aerosol case?, Appl. Optics, 45, 3367–3371, 2006.

Berg, L. K., Berkowitz, C. M., Ogren, J. A., Hostetler, C. A., Ferrare, R. A., Dubey, M. K., Andrews, E., Coulter, R. L., Hair, J. W., Hubbe, J. M., Lee, Y. N., Mazzoleni, C., Olfert, J. N., and Springston, S. R.: Overview of the Cumulus Humilis Aerosol Processing Study, Bulletin of the American Meteorological Society, 90(11), 1653–1667, doi:10.1175/2009BAMS2760.1, 2009.

Gamage, N. and Hagelberg, C.: Detection and analysis of microfronts and associated coherent events using localized transforms, J. Atmos. Sci., 50(5), 750–756, 1993.

Hair, J. W., Caldwell, L. M., Krueger, D. A., and She, C. Y.: High-spectral-resolution lidar with iodine-vapor filters: measure-

ment of atmospheric-state and aerosol profiles, Appl. Optics, 40, 5280–5294, 2001.

Hair, J. W., Hostetler, C. A., Cook, A. L., Harper, D. B., Ferrare, R. A., Mack, T. L., Welch, W., Isquierdo, L. R., and Hovis, F. E.: Airborne High Spectral Resolution Lidar for Profiling Aerosol Optical Properties, Appl. Optics, 47(36), 6734–6752, doi:10.1364/AO.47.006734, 2008.

Hostetler, C. A., Liu, Z., Reagan, J., Vaughan, M., Winker, D., Osborn, M., Hunt, W. H., Powell, K. A., and Trepte, C.: CALIOP Algorithm Theoretical Basis Document, Calibration and level 1 Data Products, PC-SCI-201, NASA Langley Research Center, Hampton, VA 23681, available online at http://www-calipso.larc.nasa.gov/resources/project_documentation.php, 2006.

Hunt, W. H., Winker, D. M., Vaughan, M. A., Powell, K. A., Lucker, P. L., and Weimer, C.: *CALIPSO* Lidar Description and Performance Assessmentm, J. Atmos. Ocean. Tech., 26(7), 1214–1228, 2009.

Jacob, D. J., Crawford, J. H., Maring, H., Clarke, A. D., Dibb, J. E., Emmons, L. K., Ferrare, R. A., Hostetler, C. A., Russell, P. B., Singh, H. B., Thompson, A. M., Shaw, G. E., McCauley, E., Pederson, J. R., and Fisher, J. A.: The Arctic Research of the Composition of the Troposphere from Aircraft and Satellites (ARCTAS) mission: design, execution, and first results, Atmos. Chem. Phys., 10, 5191–5212, doi:10.5194/acp-10-5191-2010, 2010.

Jäger, H.: Long-term record of lidar observations of the stratospheric aerosol layer at Garmisch-Partenkirchen, J. Geophys. Res., 110, D08106, doi:10.1029/2004JD005506, 2005.

King, M., Closs, J., Spangler, S., Greenstone, R., Wharton, S., and Myers, M.: EOS Data Products Handbook, Volume 1. EOS Project Science Office, Code 900, NASA/Goddard Space Flight Center, Greenbelt, MD 20771, 260 pp., available online at: http://eospso.gsfc.nasa.gov/ftp_docs/data_products_1.pdf, 2004.

Kim, S.-W., Berthier, S., Raut, J.-C., Chazette, P., Dulac, F., and Yoon, S.-C.: Validation of aerosol and cloud layer structures from the space-borne lidar CALIOP using a ground-based lidar in Seoul, Korea, Atmos. Chem. Phys., 8, 3705–3720, doi:10.5194/acp-8-3705-2008, 2008.

Liu, Z., Hunt, W., Vaughan, M., Hostetler, C., McGill, M., Powell, K.,Winker, D., and Hu, Y.: Estimating random errors due to shot noise in backscatter lidar observations, Appl. Optics, 45, 4437–4447, 2006.

Mamouri, R. E., Amiridis, V., Papayannis, A., Giannakaki, E., Tsaknakis, G., and Balis, D. S.: Validation of CALIPSO space-borne-derived attenuated backscatter coefficient profiles using a ground-based lidar in Athens, Greece, Atmos. Meas. Tech., 2, 513–522, doi:10.5194/amt-2-513-2009, 2009.

Mattis, I., Siefert, P., Müller, D., Tesche, M., Hiebsch, A., Kanitz, T., Schmidt, J., Finger, F., Wandinger, U., and Ansmann, A.: Volcanic aerosol layers observed with multiwavelength Raman lidar over central Europe in 2008–2009, J. Geophys. Res., 115, D00L04, doi:10.1029/2009JD013472, 2010.

McGill, M. J., Vaughan, M. A., Trepte, C. R., Hart, W. D., Hlavka, D. L., Winker, D. M., and Kuehn, R.:, Airborne validation of spatial properties measured by the CALIPSO lidar, J. Geophys. Res., 112, D20201, doi:10.1029/2007JD008768, 2007.

Mona, L., Pappalardo, G., Amodeo, A., D'Amico, G., Madonna, F., Boselli, A., Giunta, A., Russo, F., and Cuomo, V.: One year of CNR-IMAA multi-wavelength Raman lidar measurements in coincidence with CALIPSO overpasses: Level 1 products comparison, Atmos. Chem. Phys., 9, 7213–7228, doi:10.5194/acp-9-7213-2009, 2009.

Pappalardo, G., Wandinger, U., Mona, L., Hiebsch, A., Mattis, I., Amodeo, A., Ansmann, A., Seifert, P., Linne, H., Apituley, A., Alados Arboledas, L., Balis, D., Chaikovsky, A., D'Amico, G., De Tomasi, F., Freudenthaler, V., Giannakaki, E., Giunta, A., Grigorov, I., Iarlori, M., Madonna, F., Mamouri, R.-E., Nasti, L., Papayannis, A., Pietruczuk, A., Pujadas, M., Rizi, V., Rocadenbosch, F., Russo, F., Schnell, F., Spinelli, N., Wang, X., and Wiegner, M.: EARLINET correlative measurements for CALIPSO: first intercomparison results, J. Geophys. Res., 115, D00H19, doi:10.1029/2009JD012147, 2010.

Parrish, D. D., Allen, D. T., Bates, T. S., Estes, M., Fehsenfeld, F. C., Feingold, G., Ferrare, R., Hardesty, R. M., Meagher, J. F., Nielsen-Gammon, J. W., Pierce, R. B., Ryerson, T. B., Seinfeld, J. H., and Williams, E. J.: Overview of the Second Texas Air Quality Study (TexAQS II) and the Gulf of Mexico Atmospheric Composition and Climate Study (GoMACCS), J. Geophys. Res., 114, D00F13, doi:10.1029/2009JD011842, 2009.

Piironen P. and Eloranta, E. W.: Demonstration of a high-spectral-resolution lidar based on an iodine absorption filter, Opt. Lett., 19, 234–236, 1994.

Powell, K. A., Vaughan, M. A., Kuehn, R., Hunt, W. H., and Lee, K.-P.: Revised Calibration Strategy For The CALIOP 532-nm Channel: Part II – Daytime, Reviewed and Revised Papers Presented at the 24th International Laser Radar Conference, 1177–1180, ISBN 978-0-615-21489-4, 2008.

Powell, K. A., Hostetler, C. A., Liu, Z., Vaughan, M. A., Kuehn, R. E., Hunt, W. H., Lee, K. Trepte, C. R., Rogers, R. R., Young, S. A., and Winker, D. M.: CALIPSO Lidar Calibration Algorithms: Part I - Nighttime 532 nm Parallel Channel and 532 nm Perpendicular Channel, J. Atmos. Oceanic Technol., 26, 2015–2033, doi:10.1175/2009JTECHA1242.1, 2009.

Powell, K. A., Vaughan, M. A., Rogers, R. R., Kuehn, R. E., Hunt, W. H., Lee, K-P., and Murray T. D.: The CALIOP 532-nm Channel Daytime Calibration: Version 3 Algorithm, Reviewed and Revised Papers Presented at the 25th International Laser Radar Conference, 1367–1370, 2010.

Rienecker, M. M., Suarez, M. J., Todling, R, Bacmeister, J., Takacs, L., Liu, H.-C., Gu, W., Sienkiewicz, M., Koster, R.D., Gelaro, R., Stajner, I., and Nielsen, J. E.: The GEOS-5 Data Assimilation System - Documentation of Versions 5.0.1, 5.1.0, and 5.2.0. Technical Report Series on Global Modeling and Data Assimilation, NASA/TM-2008-104606, 27, available online at: http://gmao.gsfc.nasa.gov/pubs/tm/, 2008.

Rogers, R. R., Hair, J. W., Hostetler, C. A., Ferrare, R. A., Obland, M. D., Cook, A. L., Harper, D. B., Burton, S. P., Shinozuka, Y., McNaughton, C. S., Clarke, A. D., Redemann, J., Russell, P. B., Livingston, J. M., and Kleinman, L. I.: NASA LaRC airborne high spectral resolution lidar aerosol measurements during MILAGRO: observations and validation, Atmos. Chem. Phys., 9, 4811–4826, doi:10.5194/acp-9-4811-2009, 2009.

Russell, P. B., Swissler, T. J., and McCormick, M. P.: Methodology for error analysis and simulation of lidar aerosol measurements, Appl. Opt., 18, 3783–3797, 1979.

Russell, P. B., Morley, B. M., Livingston, J. M., Grams, G. W., and Patterson, E. M.: Orbiting lidar simulations. 1: Aerosol and cloud measurements by an independent-wavelength technique, Appl. Opt., 21, 1541–1553, 1982.

She, C. Y.: Spectral Structure of Laser Light Scattering Revisited: Bandwidths of Nonresonant Scattering Lidars, Appl. Opt., 40, 4875–4884, 2001.

Shipley, S. T., Tracy, D. H., Eloranta, E. W., Trauger, J. T., Sroga, J. T., Roesler, F. L., and Weinman, J. A.: High spectral resolution lidar to measure optical scattering properties of atmospheric aerosols. 1: Theory and instrumentation, Appl. Opt., 22, 3716–3724, 1983.

Vaughan, M., Young, S., Winker, D., Powell, K., Omar, A., Liu, Z., Hu, Y., and Hostetler, C.: Fully automated analysis of spacebased lidar data: an overview of the CALIPSO retrieval algorithms and data products, Proc. SPIE, 5575, 16–30, 2004.

Vaughan, M. A., Liu, Z., McGill, M. J., Hu, Y., and Obland, M. D.: On the spectral dependence of backscatter from cirrus clouds: Assessing CALIOP's 1064 nm calibration assumptions using cloud physics lidar measurements, J. Geophys. Res., 115, D14206, doi:10.1029/2009JD013086, 2010.

Vernier, J. P., Pommereau, J. P., Garnier, A., Pelon, J., Larsen, N., Nielsen, J., Christensen, T., Cairo, F., Thomasson, L. W., Leblanc, T., and McDermid, I. S.: Tropical stratospheric aerosol layer from CALIPSO lidar observations, J. Geophys. Res., 114, D00H10, doi:10.1029/2009JD011946, 2009.

Wandinger U. and Ansmann, A.: Experimental Determination of the Lidar Overlap Profile with Raman Lidar, Appl. Opt., 41, 511–514, 2002.

Winker, D.: Accounting for multiple scattering in retrievals from space lidar, Proc. SPIE Int. Soc. Opt. Eng., 5059, 128–139, 2003.

Winker, D. M., Hunt, W. H., and McGill, M. J.: Initial performance assessment of CALIOP, Geophys. Res. Lett., 34, L19803, doi:10.1029/2007GL030135, 2007.

Winker, D. M., Vaughan, M. A., Omar, A. H., Hu, Y., Powell, K. A., Liu, Z., Hunt, W. H., and Young, S. A.: Overview of the CALIPSO Mission and CALIOP Data Processing Algorithms, J. Atmos. Oceanic Technol., 26, 2310–2323, doi:10.1175/2009JTECHA1281.1, 2009.

Winker, D. M., Pelon, J., Coakley, J. A., Ackerman, S. A, Charlson, R. J., Colarco, P. R., Flamant, P., Fu, Q., Hoff, R. M., Kittaka, C., Kubar, T. L., LeTreut, H., McCormick, M. P., Megie, G.Poole, L., Powell, K., Trepte, C., Vaughan, M. A., and Wielicki, B. A.: The CALIPSO Mission: A Global 3D View of Aerosols and Clouds, J Bulletin of the American Meteorological Society, doi:10.1175/2010BAMS3009.1, in press, 2010.